Effect of NbMo Addition on the Precipitation Behaviour of V Microalloyed Steel during Intercritical Annealing

E. Abbasi *[1], W. M. Rainforth [2]

Department of Materials Science and Engineering, The University of Sheffield, Sir Robert Hadfield Building, Mappin Street, Sheffield S13JD, UK

Abstract

This paper reports on the precipitation behaviour and microstructural evolution in ~20% cold rolled NbMoV and V single microalloyed low carbon steels during intercritical annealing. The microstructure and precipitation behaviour were studied by optical and scanning/transmission electron microscopy and microanalysis, X-ray diffraction technique and Vickers hardness testing. After intercritical annealing, the resulting microstructure in both steels comprised acicular/ bainitic ferrite matrix with an uneven proportion of allotriomorphic ferrite and retained austenite and martensite. The average density of microalloying precipitates increased in both steels during intercritical annealing. NbV, NbMoV and V carbides were observed in the NbMoV steel, while V-carbide extensively appeared in the V steel. The results also showed a much greater precipitation strengthening in the NbMoV steel after intercritical annealing compared to the V steel. The overall findings suggested that NbMo addition could retard the growth/coarsening of microalloy precipitates with a size of lower than 15nm during the intercritical annealing.

Keywords: Microalloyed steel; Intercritical annealing; Precipitation; Acicular/bainitic ferrite.

1. Introduction

In 1967 Zackay and co-workers reported a transformation induced plasticity (TRIP) effect in CrNiMoSi high strength steels [1]. Further substantial investigations into austempering after intercritical annealing confirmed the possibility of austenite retention in the microstructure at room temperature. It has been well understood that the retained austenite, especially with a carbon content of over ~1.0 wt. %, in the microstructure leads to the TRIP effect during deformation [2]. During deformation the retained austenite transforms to martensite which increases the work hardening and the formability of steels.

The cornerstone of further developments for higher strength and ductility was laid by the introduction of a microstructure consisting of at least two different components. This enables the car makers to use thinner steel sheets, whilst still providing crash protection.

In recent years, efforts have been made to increase the dynamic energy absorption during deformation with high strain rate [3]. Studies have concentrated mostly on the microstructural development of retained austenite and bainite but less so on the precipitation of microalloying elements [4-6]. Much work has been reported about controlling microstructure and precipitation behaviour during thermomechanical treatments as a function of chemical composition. Sugimoto in 2009, reported three

* Corresponding author
Tel: +98 (0) 939 077 9163
E-mail: engabasi@gmail.com
Address: Department of Materials Science and Engineering, The University of Sheffield, Sir Robert Hadfield Building, Mappin Street, Sheffield S13JD, UK
1. PhD
2. Professor

generations of TRIP assisted steels. Their mechanical properties are strongly affected by the microstructure of the matrix. The development of the matrix in these steels is a function of thermomechanical processing and chemical composition and can be polygonal ferrite, bainitic ferrite or annealed martensite [5, 7, 8]. The coexistence of different phases requires an accurate production process and precise design of chemical composition.

The microstructure of TRIP assisted steels comprising a multiphase structure for stamping applications are widely manipulated by cold rolling and subsequent intercritical annealing, followed by austempering within the bainite temperature range.

The available data in the literature suggest that V(C, N) precipitation widely occurs in the ferrite at temperatures up to intercritical annealing range. This serves as a means for the precipitation strengthening of steels. The precipitation strengthening in microalloyed steels is markedly consistent with the volume fraction, morphology and the average diameter of precipitates.

Decreasing the number and increasing the average diameter of precipitates as a result of coarsening (Ostwald ripening) significantly reduce the effect of precipitation strengthening. The theoretical coarsening kinetics for spherical precipitates is related to the diffusion coefficient of the solute in the matrix, the interfacial energy between precipitate and matrix, the concentration of solute in the equilibrium with a precipitate of infinite radii and the molar volume of the precipitates. These parameters show that the precipitation coarsening is strongly dependent upon the microstructure and chemical composition [9-11]. Nevertheless, in a polygonal ferrite matrix it is difficult to precisely predict the precipitation strengthening due to the coexistence of softening mechanisms of recovery/recrystallisation, and active hardening mechanisms of martensite/bainite formation. The recrystallisation of polygonal ferrite can annihilate a large number of dislocations through the heating stage of intercritical annealing. This can encourage a homogeneous precipitation of microalloying elements. The question then arises if dislocations during an intercritical annealing process can enhance an intense precipitation and also to what extent they influence the growth/coarsening of precipitates.

Very limited works have been reported on the interaction between the precipitation and pipe diffusion in ferrite at intercritical annealing range [12-14]. One of the earliest works on V(C,N) precipitates in bainite was reported by Dunlop and Honeycombe in 1976 in Cr-Mo-V creep resisting steel [15]. They pointed out that the coarsening of precipitates at isothermal temperature of 700 °C is relatively sluggish. Their comparative results showed that the rate of coarsening during tempering could be ranked in descending order of ferrite ▪ martensite or bainite. However, no evidence could be found for the microstructural evolution and V(C,N) and NbMoV (C,N) precipitation behaviour during intercritical annealing in TRIP assisted steels with an acicular/bainitic ferrite matrix. Presumably, Nb containing carbo-nitrides can be formed at higher temperatures, and hence they are less soluble at intercritical annealing range [16]. The presence of Mo increases the solubility and reduces the activity of microalloying elements and C/N in austenite that enhances the precipitation in ferrite [17-19]. Moreover, Mo reduces the interfacial energy of Nb(C,N), that enhances the nucleation and suppresses the coarsening of Nb(C,N) precipitates. As the diffusion coefficient of vanadium is rather lower than carbon/nitrogen, the diffusion flux of vanadium is a rate controlling factor in the precipitation and coarsening. Therefore, in this research, the amount of carbon was used at rather low level, aiming at enhancing coarsening. This amount of carbon can also secure a proper level of retained austenite in the final microstructure [20].

In the present study, the precipitation behaviour in a slightly cold rolled bainitic/acicular ferrite matrix was investigated. A comparison was made between two precipitation systems in order to further understand the effect of NbMo addition on the microstructural evolution and precipitation behaviour in a V microalloyed steel during intercritical annealing.

2. Experimental Procedure

The chemical compositions of studied steels are shown in Table 1. These steels were produced through an identical hot/rough rolling process and are hereafter referred to as "NbMoV" and "V" steels. The amount of each element was measured by a spark Optical Emission Spectroscopy technique (OES), where the amount of nitrogen was analysed by a combustion/fusion technique.

Table 1. Chemical composition of investigated steels (wt. %).

Steel	C	Mn	Si	Al	V	Mo	Nb	N	P	S	Fe
NbMo	0.12	1.47	1.54	0.02	0.16	0.08	0.04	0.0042	0.018	0.005	Bal.
V	0.12	1.49	1.51	0.02	0.16	< 0.01	<0.01	0.0042	0.017	0.005	

In this study cold rolling (nominally 20% reduction) was carried out on both hot rolled steels. It was believed that the dislocations generated by cold rolling could enhance the precipitation during intercritical annealing [12]. Samples were cut from the cold rolled specimens in the dimension of 15x15x1 mm^3. To conduct a systematic study on the microstructural evolution and precipitation behaviour, an intercritical annealing was simulated which was followed by water quenching (Fig. 1). It is worth mentioning that the substantial work on intercritical annealing was carried out through our previous studies [21], with a focus on simulating the industrial practice undertaken by Tata Steel. An induction furnace equipped by fast heating/cooling controllable system, was used to prepare the samples in room atmosphere.
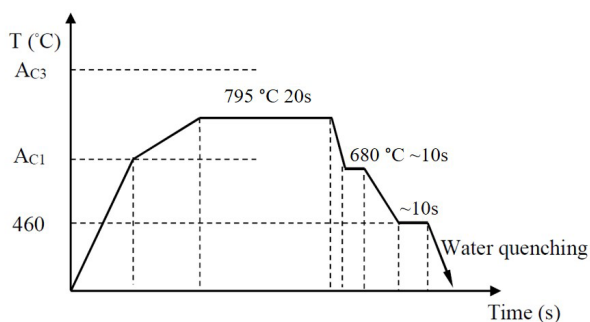

Fig. 1. Illustration of intercritical annealing schedule.

Specimens before/after heat treatment were prepared according to standard methods. The etching in a solution of 2% Nital was applied to the specimens for light optical, Scanning Electron Microscopy (SEM) and XRD testing. A FE-InspectF SEM was used to undertake secondary electron imaging at 20kV. The Energy Dispersive X-ray Spectroscopy (EDS) was also applied to micro-analyse precipitates. Further details of microstructure and precipitates were studied by conventional Transmission Electron Microscopy (TEM) through a combination of Philips EM420 at 120 kV and TECNAI-F20 at 200 kV. The TEM observations were assisted by EDS to determine the chemical composition of precipitates in thin foil and carbon extraction replica samples.

A D5000 Siemens with Co Kα radiation (i.e. including Co kα1 (λ = 0.178897 nm) and Co kα2 (λ = 0.179285 nm) radiations) was used to study the crystalline structure of studied steels according to ASTM E975–03. Rietveld refinement was performed by the Topas Academic package software V5.0 to characterize retained austenite.

The Vickers hardness was carried out according to ASTM E 92-82 using a Universal hardness by loading of 10 kgf with 20s holding time before unloading. Average hardness was determined from at least ten measurements per each sample.

3. Results
3. 1. Microstructure

Figs. 2 (a) and (b) show selected optical micrographs of cold rolled samples. From the microscopy and XRD results, it was found that the microstructure mainly comprised allotriomorphic ferrite in addition to lath ferritic constituents.

Figs. 2 (c) to (f) show the microstructure of the cold rolled samples after the intercritical annealing. A comparison between Figs. 2 (a) to (d) showed that the recrystallisation did not occur through the dark regions, i.e. acicular/bainitic ferrite and martensite. Figs. 2 (e) and (f), compare the SEM micrographs corresponding to the microstructure of secondary phases i.e. retained austenite, martensite and bainite, after the intercritical annealing of the cold rolled samples.
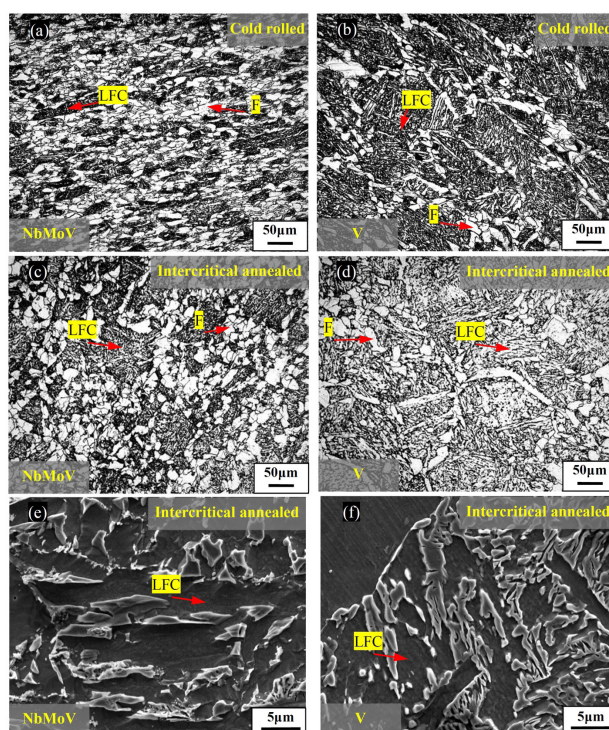

Fig. 2. Micrographs corresponding the cold rolled and intercritical annealed samples, (a) to (d) Optical micrographs, (e) and (f) SEM micrographs, F; Ferrite, LFC; Lath shaped ferritic constituents.

SEM results also showed small precipitates with an average size between 180 and 200nm after the intercritical annealing in both steels (e.g. Fig. 3). It is likely that these precipitates were formed during intercritical annealing. However, the EDS spectra did not show the peaks corresponding to the microalloying elements in these features. This was probably attributed to the relatively small size of these features compared to the interaction volume of beam.
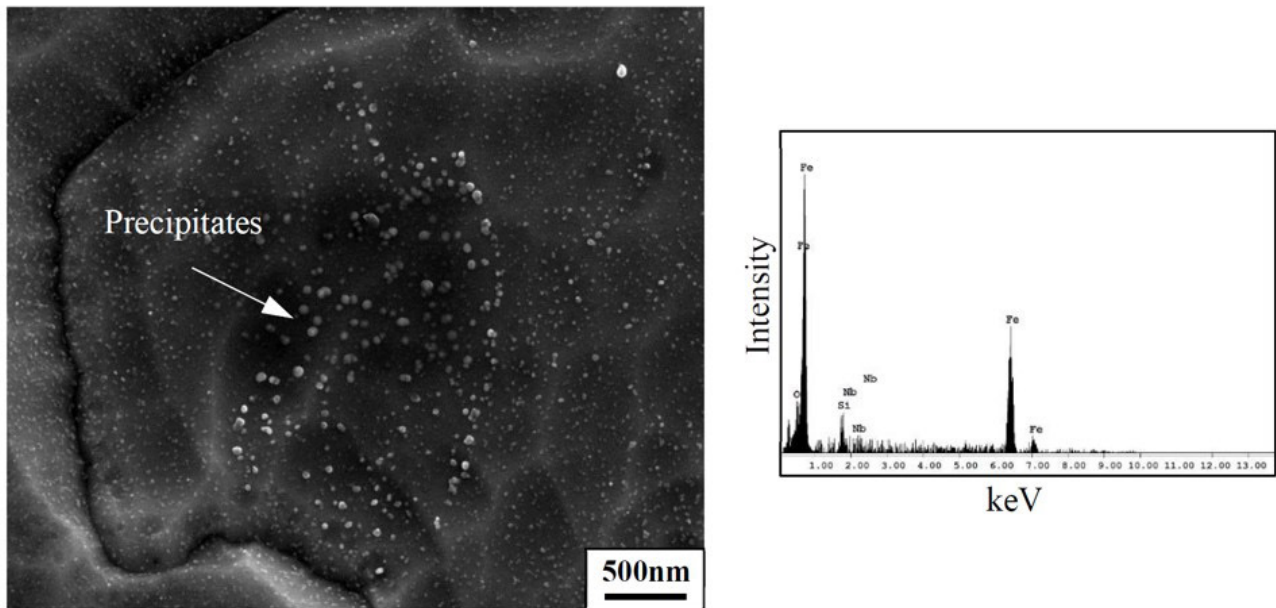
Fig. 3. Selected SEM micrograph and corresponding EDS spectrum, showing nano-scale precipitates in NbMoV steel after intercritical annealing.

Table 2. The retained austenite characteristics, measured from XRD results.

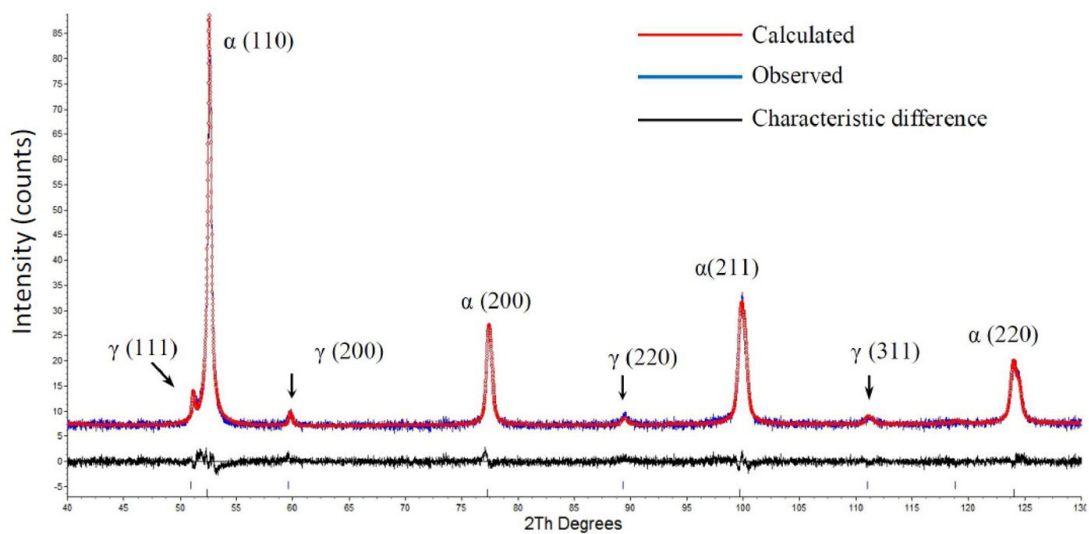| Steel	Retained austenite (Vol %)	Carbon content (%)	Lattice parameter (nm)
NbMo	7.4	1.16	0.35977±0.00019
V	8.2	1.19	0.36010±0.00009

Fig. 4. Selected XRD spectrum showing the presence of ferrite and retained austenite.

The XRD patterns of intercritical annealed samples showed two peaks corresponding to ferritic constituents (BCC-crystal structure) and retained austenite (FCC-crystal structure), e.g. Fig. 4. The characterization of retained austenite was carried out using the whole diffraction pattern. The amount of retained austenite was measured from the integrated intensity of XRD patterns. Table 2 gives the details of retained austenite in both steels. The carbon content of retained austenite was estimated using the following equation [21]:

$$a_\gamma = 0.35467 + 0.00467 \text{ wt. \%C} \qquad \text{Eq. (1)}$$

, where a_γ stands for the actual lattice parameter (nm) of retained austenite at room temperature.

3. 2. Precipitates

The TEM observations indicated the presence of precipitates with different morphologies and a wide size distribution. The precipitates were present in both steels, before and after the intercritical annealing. However, the position of precipitates, size distribution and their chemical analysis were taken into consideration to interpret the precipitation behaviour.

The analyses indicated considerable precipitation in both steels during the intercritical annealing at temperatures below ≤795 ºC. In thin foil samples, two different techniques of EDS microanalysis and dark field were applied to identify the precipitates from other unwanted sources of contrast such as a periodic contrast of dislocations, thickness fringes and oxides. Additionally, the copper and iron peaks were present in almost all of EDS spectra. The observed copper peaks are due to the copper grid and TEM holder and the Fe peaks in replica samples arises from the extraction of iron from the substrate.

Fig. 5 shows TEM micrographs corresponding to microalloying containing precipitates in thin foil samples of both steels. It is believed that increasing the temperature up to the intercritical range (i.e. 795 ºC) might lead to recovery in the microstructure [22, 23]. Interestingly, despite the high possibility of recovery, the EDS microanalysis revealed the presence of V and (Nb,Mo,V) containing precipitates through regions with a high dislocation density. The dislocation density in both steels was generally low, although accumulations of dislocations at the corner of grain boundaries were occasionally observed (Fig. 5 (b)).

Moreover, precipitates were observed inside the martensite and retained austenite in both steels (Fig. 5). It is likely that the observed martensite arose from

transformation of the fresh austenite during the quenching stage of intercritical annealing. Fig. 5 (g) gives a typical micrograph of retained austenite after the intercritical annealing. Micrographs and EDS results confirmed the presence of microalloying precipitates inside and at places close to the edge of retained austenite and with annealing twinning.

According to the bright/dark field TEM images, the carbon extraction replicas successfully extracted the precipitates larger than about 5 nm (e.g. Fig. 6). Note that TEM micrographs show a projected image from the 3D configuration of precipitates. However, a wide range of size and shape distribution of precipitates and also chemical compositions were frequently observed (e.g. Fig. 6). The EDS spectra from these carbides confirmed the presence of different microalloying elements i.e. Nb/V and Mo in NbMoV steel. According to the TEM micrographs and the relevant EDS results, it can be suggested that during the thermomechanical processing
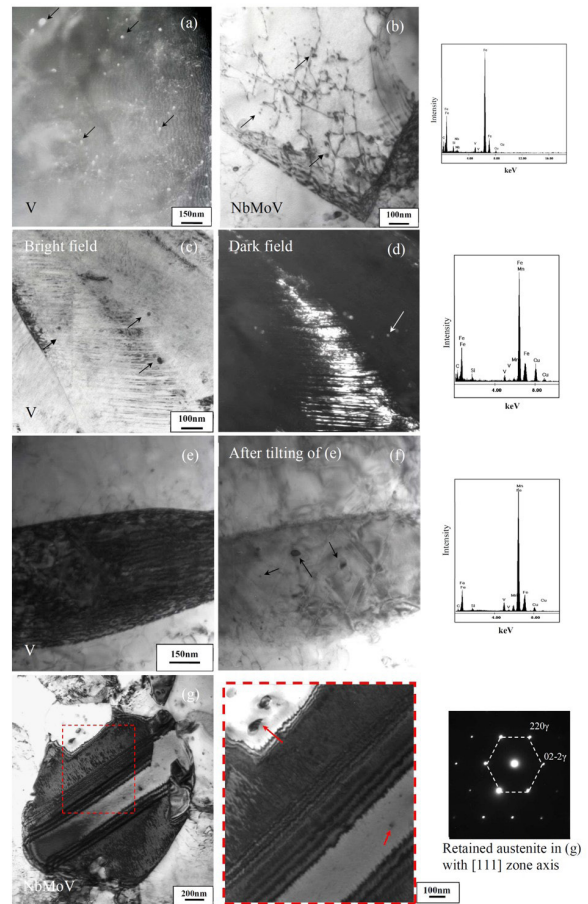

Fig. 5. Typical TEM micrographs and EDS spectra of thin foil samples, showing the presence of nano-scale microalloy precipitates in the microstructure after intercritical annealing (arrows indicate precipitates).

nano-scale precipitates of Nb/V/Mo/Ti containing with a cuboid, spherical, needle-like/oval and complex shaped were formed. For example, Fig. 7 shows TEM micrographs and corresponding EDS spectra of a typical complex precipitate. The dark field images of upper and lower caps are strong evidence showing different crystallographic orientations of duplex precipitates. In this way, the EDS spectra acquired from the upper and lower caps showed that the lower cap is rich in Nb,V,Ti, where upper cap is rich in Nb. It has been established that the cap can be formed first in a fully austenitic region and acts as nucleation sites for the subsequent precipitation at lower temperatures [24, 25]. The significant difference between the size of upper and lower caps suggests that Nb,V,Ti was probably formed at a higher temperature.

The average density of precipitates was measured by counting the number of precipitates through the carbon extraction replica micrographs (i.e. number of precipitate per unit area), obtained from at least ten negatives for each sample. Fig. 8 compares the average density of precipitates, before and after the intercritical annealing. However, TEM observations suggested that the frequency of precipitates in terms of their morphology did not change significantly after intercritical annealing in both steels. It can be seen that the intercritical annealing significantly increased the density of precipitates in both steels.
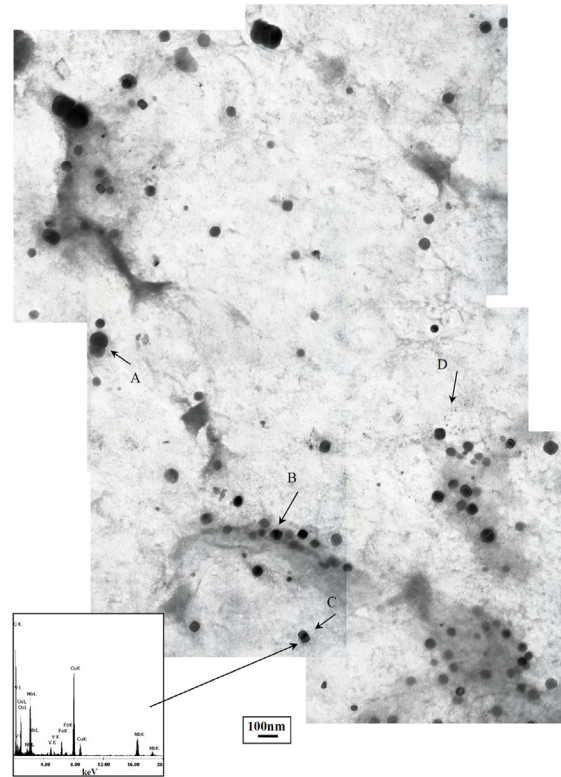

Fig. 6. Selected carbon extraction replica micrograph and EDS spectrum, showing microalloy precipitates in NbMoV steel after intercritical annealing, A; complex shaped, B; round shaped, C; square shaped; D; fine precipitates.
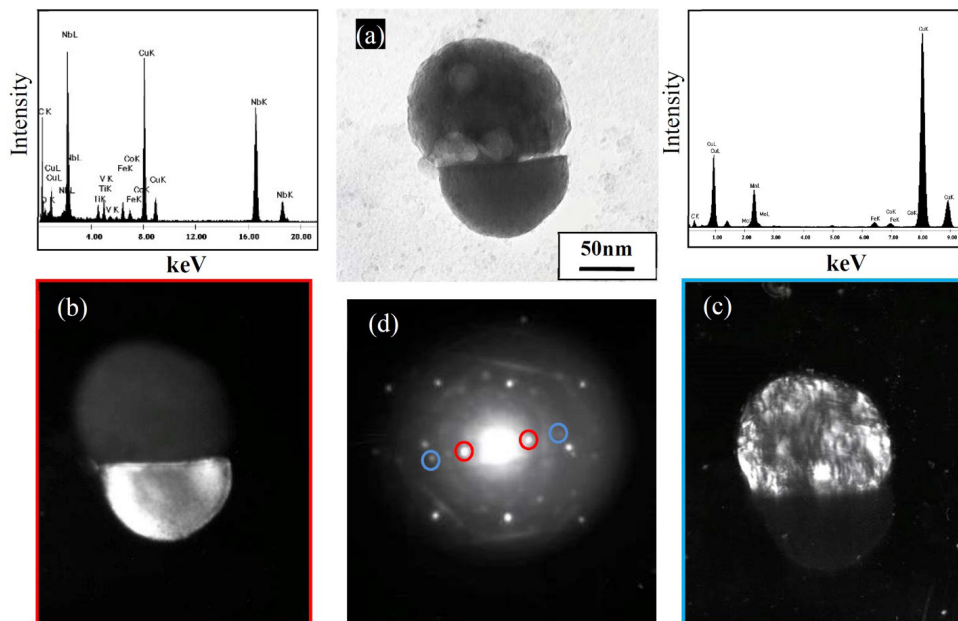

Fig. 7. Selected carbon extraction replica micrograph of NbMoV steel, (a) Bright field image of a complex NbV precipitate, (b) and (c) Showing the dark field images of upper and lower caps and corresponding EDS spectra, respectively, (d) Electron diffraction pattern showing the relevant variants of each cap.
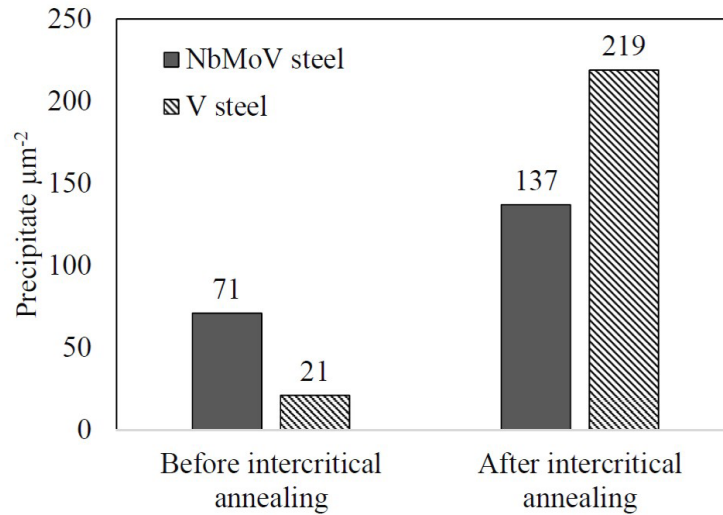
Fig. 8. The number of microalloy precipitates per unit area (average density), measured from the carbon extraction replica samples of NbMoV and V steels.

Fig. 9 gives the size distribution of precipitates (comparative histograms corresponding to the precipitate size) in V and NbMoV steels. The comparative histogram shown in Fig. 9 (a) indicates the formation of a considerable fraction of fine precipitates (i.e. ≤15 nm) in NbMoV steel. On the other hand, in V steel the histogram exhibits that precipitates became marginally larger than those before intercritical annealing (Fig. 9 (b)). Additionally, a comparison between the histograms of NbMoV and V steels after intercritical annealing

showed that the frequency of fine precipitates (i.e. ≤15 nm) was higher in the former steel (Fig. 9 (c)).

3. 3. Hardness

Fig. 10 shows the trend of hardness variation after hot/ rough rolling, cold rolling and intercritical annealing. In NbMoV steel, the hardness in all specimens is higher than V steel. The results also showed that the intercritical annealing resulted in an increase in the hardness, while the
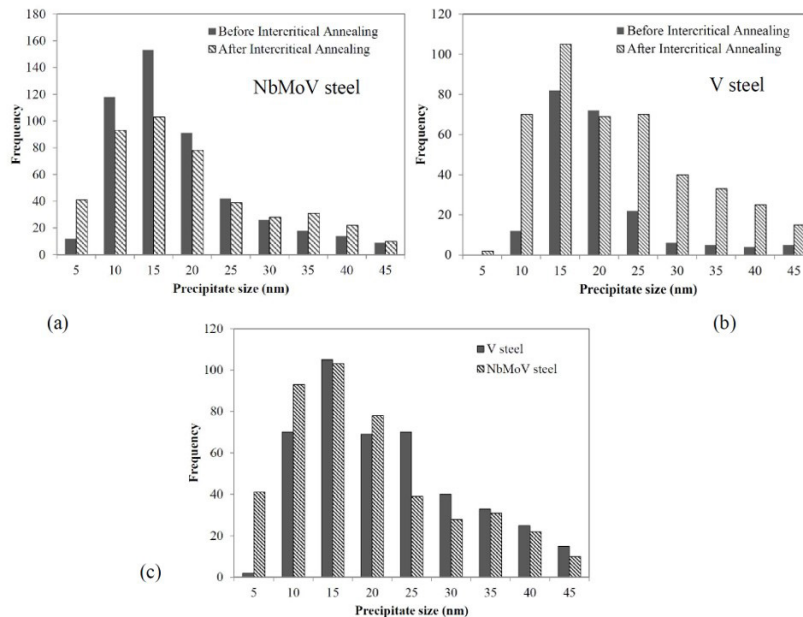

Fig. 9. Precipitate size distributions of NbMoV and V steels, (a) and (b) Before and after intercritical annealing in NbMoV and V steels, respectively, (c) After intercritical annealing of V and NbMoV steels.
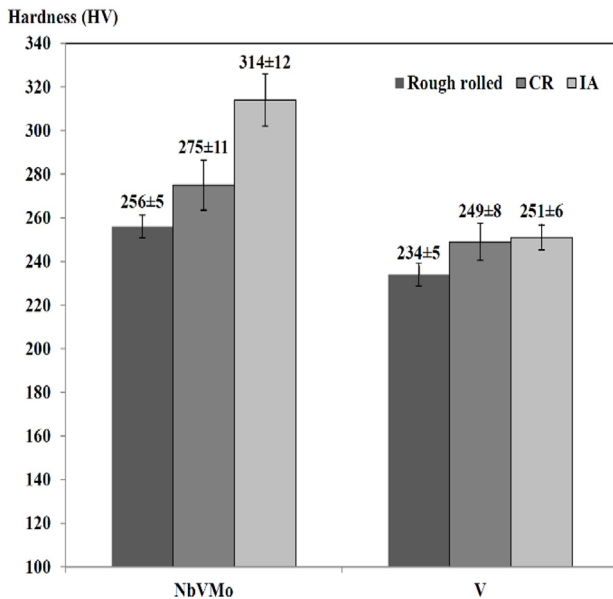
Fig. 10. Vickers hardness of NbMoV and V steels, after rough/hot rolling, cold rolling (CR) and intercritical annealing (IA).

rate of hardening is different between NbMoV and V steels.

4. Discussion
4. 1. Microstructure

From the optical micrographs of samples before intercritical annealing, it was found that the prior hot rolling process favoured the formation of allotriomorphic ferrite and lath-shaped ferritic constituents (Fig. 2). In general, the regions in- between allotriomorphic ferrite exhibited a microstructure similar to that reported in [26, 27] for typical bainitic ferrite steels (Fig. 2). It has been established that the microstructure of such steels involves a matrix of bainitic ferrite lath and interlath packets of retained austenite and martensite. In the present study, a combination of SEM/TEM observations and XRD results revealed the presence of acicular/bainitic ferrite and martensite with a high dislocation density at these regions. It is therefore clear that the matrix of both steels mainly comprised acicular/bainitic ferrite and martensite.

After the intercritical annealing the optical micrographs revealed an allotriomorphic ferrite at prior austenite grain boundaries and a distribution of lath shaped ferritic constituents at grain interiors (Figs. 2 (c) and (d)). This is similar to that observed in the optical micrographs of initial structure (Fig. 2). Of particular note was that the lath shaped ferrite did not show any significant recrystallisation after intercritical annealing. This is in agreement with the results of Sugimoto et al. and other

researchers who reported no significant nucleation of polygonal ferrite after intercritical annealing of a given (0.1-0.6)C 1.5Si 1.5Mn (wt. %) martensitic TRIP steel 8). Recently, Hamzeh et al., and Hossein Nedjad et al., have published similar results about the effect of cold rolling on the formation of an ultrafine ferrite grain size microstructure in bainitic microstructures after an annealing process at 500-700 ºC. It was pointed out that heavy cold rolling (i.e. ≥50% reduction) can break bainitic structures and enhance ferrite recrystallisation. From the microscopy observations in this study and available data in the literature, it can be thus suggested that the cold rolling reduction of ~20% cold rolled reduction was insufficient to drive ferrite recrystallization [28, 29].

A possible explanation about the absence of recrystallisation in the lath ferrite is deduced by assuming the effect of interfaces. It is generally accepted that the parallel sides of lath shaped ferritic constituents are low-energy, coherent or semicoherent boundaries and therefore immobile [30-32]. It is evident that the existence of such a structure necessitates a higher level of energy for the recrystallisation. This is consistent with the results of Ueji et al. in 2002 who discovered that ~50% plastic strain in a martensitic microstructure leads to subdivision of martensite laths. They showed that introduced heterogeneous subdivisions provide ideal potential sites for the formation of new grains [33].

Nevertheless, the optical micrographs of V steel revealed a slight coarsening of lath ferritic constituents compared with NbMoV steel (Figs. 2 (c) and (d)). This behaviour could be attributed to the effect of NbMo addition in retarding the ferrite growth by pinning the grain boundaries as precipitate or solute drag effect.

4. 2. Precipitates

A comparison between the TEM observations of the initial and intercritical annealed structures showed that the initial structure as well as final structure contained a large density of dislocations (e.g. Fig. 5). This was good evidence to show that the precipitation and coarsening would be significantly influenced by dislocations during intercritical annealing.

TEM observations showed that the prior hot rolling process led to the formation of a considerable amount of microalloying precipitates in a random manner with different morphologies in both steels. In addition, a high frequency of VC and Nb(V,Mo)C precipitates were observed in the tangle of dislocations and also in the grain boundaries of ferritic constituents after the intercritical annealing (e.g. Fig. 5). The available results suggested that the dislocations/grain boundaries as short circuit

diffusional paths would accelerate the formation and coarsening of precipitates during intercritical annealing. It was also possible that many of the precipitates initially formed in the supersaturated ferrite and then dislocations were generated as result of transformation. On the other hand, a possibility exists that precipitates might enhance the generation of dislocations [16]. However, these results point to the fact that the precipitates increase the strength of steel by precipitation strengthening. These effects will be further clarified through the following section.

Twinned martensite adjacent to VC and other Nb(V,Mo)C precipitates was occasionally observed (e.g. Figs. 5 (c) and (e)). These results showed the possibility of precipitation in austenite at temperatures up to intercritical annealing range. Therefore, it was likely that precipitates locally had depleted the carbon and consequently reduced the stability of retained austenite against martensite transformation. Nevertheless, if the twinned martensite and other planar defects were not formed during intercritical annealing they could accelerate the coarsening of pre-existing precipitates.

As a general conclusion, precipitates formed in the matrix, on dislocations and at the grain boundaries of polygonal/lath ferrite (e.g. Fig. 5). The location of precipitates provided good evidence to show the preferential potential sites for the formation and coarsening of precipitates. Moreover, these characterizations suggested that the statistical studies on the density of precipitates cannot be considered for a homogeneous distribution of precipitates in these microstructures. However, the following discussions will be made based on the average of densities of precipitates from different micrographs.

From the TEM analysis, it was also found that the average density of precipitates increased after intercritical annealing in both steels (Fig. 8). This is comparable to other reports in the literature about the precipitation of V(C,N) precipitates in TRIP steels with a polygonal ferrite matrix during intercritical annealing [34, 35]. This simply means that during intercritical annealing further precipitation occurred in both steels.

Fig. 6 showed typical precipitate morphologies in the intercritical annealed samples. It is clear that during the prior hot rolling and intercritical annealing, precipitates with different sizes and morphologies (i.e. namely spheroid, cuboid, oval, triangle and irregular/complex shaped) were formed. It has been established in the literature that differences in the size and morphology of precipitates is generally attributed to the composition, the nucleation temperature, the mechanism of growth and subsequent coarsening [36, 37]. The growth/coarsening of precipitates depends on the chemical composition, microstructure and heat treatment parameters [9]. The

kinetics of growth and coarsening are mainly influenced by volume and pipe diffusion. On the other hand, the level of coherency can greatly affect the morphology of precipitates [38]. However, no evidence was found to link the precipitate morphology and precipitate size in the present study.

A few precipitates with a size of between ~50 to 200nm were also observed in replica samples, in particular in NbMoV steel with a chemical composition of Nb(V,Mo)C (e.g. Fig. 7). It is believed that these precipitates either did not dissolve during the reheating stage or they formed at high temperatures. This is consistent with the findings of Palmiere et al. who showed that the dissolution temperature of multi-microalloying precipitates is higher than simple Nb carbide [25]. However, it is believed that this group of precipitates do not greatly contribute to precipitation strengthening [37].

Fig. 9 showed that ~80% of precipitates in both steels in the hot rolled and in NBMoV steel in the intercritical annealed condition, were smaller than 20nm. It has been established that the precipitates with a size of less than approximately 15nm are mainly responsible for the strengthening [11, 37]. Therefore, the frequency of precipitates at this range was considered more closely in the following.

The TEM observations and EDS analysis suggested that the majority of precipitates in NbMoV steel comprised NbVC and Nb(VMo)C before intercritical annealing. There is no extensive literature about the precipitation behaviour of co-precipitation system of Nb(VMo)(C,N). However, Akben et al.'s studies of austenite recovery and recrystallisation in Nb and V microalloyed steels showed that the recrystallisation in Nb containing steels is stopped at higher temperatures compared with V added steels 39). They suggested that the austenite recrystallisation-stop temperature is related to the solute drag effect and carbonitride precipitates. Therefore, it was assumed that a large number of Nb(V,Mo)C precipitates in NbMoV steel have been formed at higher temperatures, (i.e. probably around ≥900 ºC).

It has been established that the less soluble precipitates generally coarsen more slowly than more soluble ones [40]. Detail studies on the precipitation behaviour of NbMoV and V steels during hot rolling process have been published elsewhere [41]. It was shown that a noticeable number of precipitates in NbMoV steel, as opposed to V steel, are formed at temperatures over 830 ºC. According to the classical theory this suggests that the Nb(V,Mo)(C,N) precipitates presumably tend to coarsen more slowly than V(C,N) during intercritical annealing [16]. The validity of this assumption will be discussed next.

The histograms shown in Fig. 9 (c) suggest that the

precipitates in V steel were marginally larger than those in NbMoV steel after intercritical annealing, although the difference was not large and not necessarily statistically meaningful. Since most of precipitates in NbMoV steel showed a chemical composition of Nb(V,Mo)C, it is suggested that NbMo addition could control the coarsening of precipitates during the process. Similarly, Balliger and Honeycombe showed that the kinetics of coarsening in V(C,N) interphase precipitates in ferrite at 740 ºC is rather sluggish over a critical size (i.e. ~20 to 40 nm) [12]. However, these results gave further insight into the kinetics of Nb(V,Mo)C and VC precipitation growth and coarsening in random manner in acicular/bainitic ferrite steels. Also, the results showed that the majority of precipitates grew to a size of 10 and 15nm whereas they did not tend to coarsen further during the intercritical annealing.

Note that the precipitate size distribution is based on the ferrite diameter of precipitate, whereas TEM observations showed different morphologies of precipitates in the microstructure. In general, the different morphologies of precipitates arise from the interfacial energy between the precipitates and substrate [38]. Thus, the growth/coarsening of spherical precipitates is perhaps different from the precipitates with other morphologies. However, this cannot be explained based on the available data and further investigations would be required to better understand this behaviour.

4. 3. Hardness

A comparison between hardness measurements (Fig. 10) showed a higher hardness in both steels after the cold rolling, as expected (i.e. 275±11 and 249±8 HV in NbMoV and V steels, respectively). An alternative explanation is attributed to the work hardening and subdivision of grains in allotriomorphic ferrite in the microstructure of cold rolled specimens.

The trend of hardness variation in Fig. 10 showed the marked effect of intercritical annealing in increasing the hardness in NbMoV steel, whereas V steel exhibited no significant change (i.e. 314±12 and 251±6 HV in NbMoV and V steels, respectively). The increase in hardness in NbMoV steel is believed to be associated with precipitation as well as bainite/martensite transformation [42, 30]. This is supported by TEM observations, which showed an increase in the number of precipitates and a retention of a high dislocation density in NbMoV steel. By contrast, this behaviour was more complex in V steel, as the hardness did not significantly increase due to the possible precipitation of vanadium carbide. Based on the available data, two possible explanations can be offered. Firstly, the possible relaxation and growth of acicular/bainitic ferritic and tempered martensite and variations in the volume fraction of bainite/martensite could neutralise the

possible precipitation strengthening. Another explanation lies in the coarsening of very fine precipitates (probably with a size of ≤5 nm). This seems reasonable as the average density of precipitates (with diameter of ≥5 nm) increased, whereas no significant variation was observed in the hardness and size distribution of precipitates. Moreover, it can be concluded that the lower rate of coarsening of precipitates in NbMoV steel was due to the effect of NbMo, which resulted in an increased hardness despite the average density of precipitates is being lower than in V steel.

5. Conclusions

NbMoV steel has a similar composition to V steel, except it has the addition of 0.08%Mo and 0.04%Nb, which is expected to promote the additional precipitation of Nb(C,N) type precipitates during thermomechanical processing. This steel was used, to investigate the effect of the microstructural evolution and precipitation coarsening. The findings and conclusions that can be drawn are summarised as follows:

•　Both steels showed an acicular/bainitic ferrite matrix surrounded by allotriomorphic ferrite after ~20% cold rolling and intercritical annealing. Also, the lath ferritic constituents failed to recrystallise during intercritical annealing in both steels.

•　After intercritical annealing the density of precipitates in V steel raised over NbMoV steel (i.e. 137 and 219 precipitate μm-2 in NbMoV and V steels, respectively). This was attributed to the greater kinetics of V(C,N) precipitation than (Nb,V,Mo)(C,N) system at this range of temperature.

•　The rate of growth/coarsening of precipitates, in particular with a size of ≤15nm, in NbMoV steel was lower than V steel after intercritical annealing. This was attributed to the effect of Nb and Mo on retarding the growth/coarsening of precipitates during intercritical annealing range.

•　The NbMoV steel showed higher hardness after intercritical annealing, whereas the hardness in V steel was not significantly changed. This was mainly attributed to the effect of precipitation strengthening of precipitates with a size of ≤15nm.

•　Very few microalloying precipitates were observed in the intercritical annealed austenite, adjacent to martensitic regions. This suggested that the carbo-nitrides could locally reduce the stability of austenite against martensite transformation.

References

[1] V. F. Zackay, E. R. Parker, D. Fahr and R. Busch: Trans. ASM., 60(1967), 252.
[2] E. Abbasi, Q. Luo and D. Owens: Mater. Sci. Eng. A., 725(2018), 65.

[3] B. C. De. Cooman: Curr. Opin. Solid State Mater. Sci., 8(2004), 285.

[4] S. Allain and T. Iung: Rev. DE Metallurgie-Cahiers D Inf. Technol., 105(2008), 520.

[5] K. I. Sugimoto, Mater. Sci. Technol., 25(2009), 1108.

[6] A. Halder; S. Suwas; D. Bhattacharjee: Proc. Int. Conf. on Microstructure and Texture in Steels and Other Materials., Jamshedpur, 2008.

[7] T. Hojo, K. I. Sugimoto, Y. Mukai and S. Ikeda: ISIJ Int., 48(2008), 824.

[8] K. I. Sugimoto, A. Kanda, R. Kikuchi, S. I. Hshimoto, T. Kashima and S. Ikeda, ISIJ Int., 42(2002), 910.

[9] G. L. Dunlop and R. W. K. Honeycombe: Philos. Mag., 32(1975), 61.

[10] A. Kostryzhev, N. Singh, L. Chen, Ch. Killmore and E. Pereloma: Metals., 8(2018), 134.

[11] T. N. Baker: Ironmaking Steelmaking., 43(2016), 264.

[12] R. N. K. Balliger, Met. Sci., 14(1980), 121.

[13] D. P. Dunne: Mate. Sci. Technol., 26(2010), 410.

[14] H. J. Kestenbach: Mater. Sci. Technol., 13(1997), 731.

[15] G. L. Dunlop and R. W. K. Honeycombe: Met. Sci., 10(1976), 124.

[16] T.Gladman: The physical metallurgy of microalloyed steels, Maney Publishing for the Institute of Materials, 2002.

[17] J. H. Jang, Y. U. Heo, C. H. Lee, H. K. D. H. Bhadeshia and D. W. Suh: Mater. Sci. Technol., 29(2013), 309.

[18] X. Sun and Q. Yong: Int. Seminar on Applications of Mo in Steels, Beijing, 2010.

[19] C. M. Enloe, K. O. Findley, C. M. Parish, M. K. Miller, B. C. De-Cooman and J. G. Speer: Scripta Mater., 68(2013), 55.

[20] J. Naitou, T. Murakami, Sh. Ikeda and K. Okita: Patent US 2014/0044585 A1, 13 Feb 2014.

[21] E. Abbasi and W. M. Rainforth: Mater. Sci. Eng. A., 651(2016), 822.

[22] M. D. Meyer, D. Vanderschueren, K. D. Blauwe and B. C. De-Cooman: in Mechanical Working and Steel Proc. Conf., (1999).

[23] T. Siwecki, J. Eliasson, R. Langneborg and B. Hutchinson: ISIJ Int., 50(2010), 760.

[24] J. O. W. B. S. Zaefferer: Acta Mater., 52(2004), 2765.

[25] M. A. Altuna, A. Iza-Mendia and I. Gutierrez: Metall. Mater. Trans. A., 43A(2012), 4571.

[26] R. M. Poths, R. L. Higginson and E. J. Palmiere: Scripta Mater., 44(2001), 147.

[27] K. I. Sugimoto, J. Sakaguchi, T. Iida and T. Kashima: ISIJ Inter., 40(2000), 920.

[28] T. Furuhara, T. Yamaguchi, G. Miyamoto and T. Maki: Mater. Sci. Technol., 26(2010), 392.

[29] A. A. M. Hamzeh: Mater. Sci. Eng. A., 593(2014), 24.

[30] Y. M. A. V. H. M. A. S. Hossein Nedjada: Mater. Sci. Eng. A., 528(2011), 1521.

[31] H. K. D. H. Bhadeshia and R. Honeycombe: Steels Microstructure and Properties, Third ed., Elsevier Ltd., (2003), 25.

[32] L. R. H. R. Abbaschian: Physical Metallurgy Principles, Fourth Edition ed., Cengage Learning, (2009).

[33] M. F. J. Humphreys: Recrystallization and Related Annealing Phenomena, Second, Ed., Elsevier, (2004).

[34] N. Y. Y. R. Ueji: Acta Mater., 50(2002), 4177.

[35] C. Scott, F. Perrard and P. Barges: Int. Seminar 2005 on Application Technologies of Vanadium in Flat – Rolled Steels, Suzhou, China, 2005.

[36] N. K. Balliger and R. W. K. Honeycombe: Metall. Trans. A., 11A(1980), 421.

[37] T. N. Baker: Mater. Sci. Technol., 25(2009), 1083.

[38] D. A. Porter, K. E. Easterling and M. Y. Sherif: Phase Transformations in Metals and Alloys, Third ed., CRC press, (2009).

[39] M. G. Akben, B. Bacroix and J. J. Jonas: Acta Metall., 31(1983), 161.

[40] R. W. K. Honeycombe: Fundamental Aspects of Precipitation in Microalloyed Steels, in Metallurgy and Applications, (1986).

[41] T.Gladman: Mater. Sci. Techn., 15(1999), 30.